Hindawi
Advances in Civil Engineering
Volume 2018, Article ID 6940532, 8 pages
https://doi.org/10.1155/2018/6940532

Research Article

Stress-Strain Behavior of Steel Fiber-Reinforced Concrete Cylinders Spirally Confined with Steel Bars

Bambang Sabariman,[1,2] **Agoes Soehardjono**,[1] **Wisnumurti Wisnumurti**,[1] **Ari Wibowo**,[1] **and Tavio Tavio**[3]

[1]*Department of Civil Engineering, Universitas Brawijaya, Malang, Indonesia*
[2]*Department of Civil Engineering, Universitas Negeri Surabaya, Surabaya, Indonesia*
[3]*Department of Civil Engineering, Institut Teknologi Sepuluh Nopember (ITS), Surabaya, Indonesia*

Correspondence should be addressed to Tavio Tavio; tavio_w@yahoo.com

Received 29 December 2017; Accepted 26 April 2018; Published 12 June 2018

Academic Editor: Xuhao Wang

The compressive strength of concrete according to certain codes can be based on the compressive strength of unconfined plain standard concrete cylinders tests at the age of 28 days. In this paper, the standard concrete cylinders were spirally confined with steel bars and with/without hooked-end steel fibers. The influence of the use of hooked-end steel fiber in spirally confined concrete with various pitches was investigated. It can be seen that the use of hooked-end steel fiber contributes significantly in improving both compressive strength and ductility of concrete. The compressive strength and ductility of steel fibered concrete also increase with the reduction of the spiral's pitch.

1. Introduction

It has been widely reported from the results of several researches that the effects of confinement in concrete can increase its axial compressive strength and ductility. This is due to the presence of the lateral compressive force provided by the confining steel in concrete. In addition, the lateral stress acting on the concrete also increases the ductility of concrete. The lateral expansion of concrete core is confined by the lateral pressure produced by the lateral confinement steel such that the slope of the descending postpeak branch of the stress-strain curve of confined concrete decreases with the increase of confinement degree.

The use of confinement in concrete core is intended to increase ductility. The resistance generated by the transverse reinforcement is influenced by, among others, the percentage of transverse reinforcement, the strength of transverse reinforcement, the compressive strength of concrete, the spacing of transverse reinforcement, and the configuration of transverse reinforcement in concrete.

The stress-strain relationship of concrete should be discovered for its characteristics, since it can be used to derive its analytical approach or model. Several studies on the issue have been well addressed and studied previously [1–18]. The studies resulted in the stress-strain relationships of normal- and high-strength concrete as well as the stress-strain relationships of steel fiber-reinforced concrete (SFRC). From these studies, the complete analytical stress-strain relationships were obtained which include the pre- and post-peak responses of the curve. These proposed stress-strain relationships can be used further by an engineer for designing the concrete members. Both the use of confinement and steel fiber might increase the ductility of concrete. To further improve the ductility of concrete, the simultaneous effect of combined lateral confining steel and steel fibers needs to be investigated to observe its actual compressive stress-strain behavior [11–18].

Confinement in concrete can be in the forms of rectilinear or square hoops/stirrups or spiral. By laterally confining the concrete core with rectilinear or square hoops/stirrups or spiral, the increases in terms of compressive strength and ductility of concrete can be expected. The confinement serves to reduce the lateral expansion of concrete core and delay the crushing of concrete, thus further affecting the compressive

strength and ductility of concrete. Spiral provides better continuous confining pressure on concrete core, whereas the rectilinear or square hoops/stirrups provides effective confining effect at the corners since the four sides of the hoops/stirrups tend to bend outwards. Although, it is not as good as the spiral in providing effective confining effect on concrete core, the rectilinear or square hoops/stirrups can still improve the compressive strength and ductility of concrete core significantly. Thus, this type of confinement is still adopted to be used for rectangular or square concrete cross sections to provide confinement to concrete core and thus improve its ductility.

Ou et al. [17] have observed the compressive behavior of SFRC with reinforcing index (RI) up to 1.7. When RI is greater than 1.7, the compressive strength of steel fiber-reinforced concrete (SFRC) starts to degrade. Ou et al. [17] concluded that the addition of steel fiber in concrete improves the compressive strain and peak stress of SFRC significantly. However, the increase was only up to volume of fiber in concrete (V_f) of 2 percent.

Liu [18] showed that the use of hooked-end steel fiber with the dimensions of 35×0.55 mm in concrete can control better its compressive failure (better performance/ductility). However, Oliveira Júnior et al. [15] indicated that the compressive strength of unconfined concrete with hooked-end steel fiber is comparable with that of the unconfined concrete without steel fiber. They also found that the addition of steel fiber in concrete does not increase its compressive strength [15]. The slightest descending slope and the longest ultimate strain of SFRC were found at V_f equal to 2 percent.

Several proposed models [11, 13, 16, 17] related to the use of steel fiber in concrete are given as follows:

Ezeldin and Balaguru [11]:

$$\begin{aligned} f'_{cf} &= f'_c + 3.51\text{RI}\,(\text{MPa}), \\ \varepsilon_{pf} &= \varepsilon_{co} + 446 \times 10^{-6}. \end{aligned} \tag{1}$$

Nataraja et al. [13]:

$$\begin{aligned} f'_{cf} &= f'_c + 2.1604\text{RI}\,(\text{MPa}), \\ \varepsilon_{pf} &= \varepsilon_{co} + 0.0006. \end{aligned} \tag{2}$$

Ou et al. [17]:

$$\begin{aligned} f'_{cf} &= f'_c + 2.35\text{RI}\,(\text{MPa}), \\ \varepsilon_{pf} &= \varepsilon_{co} + 0.0007\text{RI}, \\ \text{RI} &= \frac{W_f L_f}{D_f}. \end{aligned} \tag{3}$$

Soroushian and Lee [16]:

$$\begin{aligned} f'_{cf} &= f'_c + 3.6 I_f\,(\text{MPa}), \\ \varepsilon_{pf} &= 0.0007 I_f + 0.0021, \\ I_f &= \frac{V_f L_f}{D_f}, \end{aligned} \tag{4}$$

where f'_{cf} is the compressive peak strength of SFRC, f'_c is the compressive peak strength of non-SFRC, RI is the reinforcement index by fiber weight, ε_{pf} is the strain corresponding to the peak stress of SFRC, ε_{co} is the strain corresponding to the peak stress of non-SFRC, W_f is the fiber weight, L_f is the fiber length, D_f is the fiber diameter, I_f is the fiber reinforcement index, and V_f is the fiber volume.

All the above studies have not explored the use of combined spiral as confinement and steel fiber in concrete. This study focuses on the compressive behavior of concrete considering the contribution of both spiral and steel fiber. Based on Oliveira Júnior et al. [15], Ou et al. [17], and Liu [18], the study investigated further on the effect of combined spiral confinement and steel fiber on the compressive behavior of concrete. There are two main findings of the study. First, the compressive strength of concrete with and without steel fiber is similar, that is, 23.0981 and 23.2634 MPa, respectively. This confirms the study by Oliveira Júnior et al. [15]. Second, the combination of spiral and steel fiber improves both the compressive strength and the strain (strain at peak strength and ultimate strain) significantly.

2. Experimental Program

2.1. Material and Mix Design. The designed compressive strength of normal-weight concrete (f'_c) was 22.5 MPa. Both the coarse and fine aggregates used for concrete satisfied the standard mix design requirements. The concrete was made in the hot weather condition, and thus, it required the addition of retarder to delay the setting time during the casting and compaction. Steel fiber was also added in some of the concrete mixture to study its effect on concrete properties compared to those without steel fiber. Superplasticizer was also used to improve its workability. The physical and mechanical properties of steel fiber used in the study are shown in Figure 1. The concrete mixture proportion obtained from the mix design is listed in Table 1. According to Figure 1 and Table 1, the value of I_f can be calculated as $I_f = V_f L_f / D_f = 1.60$.

2.2. Concrete Confinement. Since the application and effectiveness of spiral as confinement in concrete have been widely studied and well established both analytically and experimentally, the study concentrates mainly on the use of combination of both spiral and steel fiber together to know their interaction impact on the compressive behavior of concrete. When used together, the compressive behavior of concrete is considerably influenced by the combination of confining steel bars (spiral) and steel fiber. These two parameters were observed in the study. The size of the specimen, diameter of spiral, compressive strength of concrete, pitch of spiral, yield strength of spiral, and volumetric ratio of spiral are the parameters required to determine the value of Z_m of modified Kent–Park [12] (given by (5)–(8)). Several Z_m values were set (discussed further in Section 2.2) to study the combined effect of spiral confinement and steel fiber in

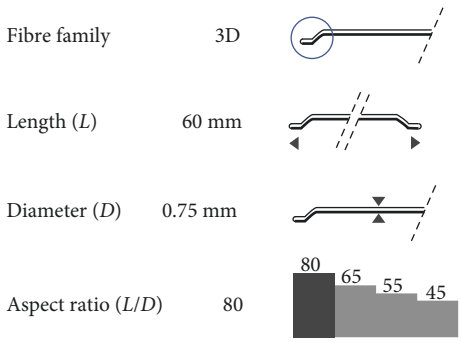

Figure 1: Physical and mechanical properties of steel fiber used in the study: tensile strength $R_{m,nom} = 1225\ N/mm^2$; tolerances ±7.5% average; Young's modulus ±210000 N/mm^2.

Table 1: Concrete mixture proportion from mix design.

Material	Volume = 0.05 m^3
Cement	10.30 kg
Fly ash (Paiton, Indonesia)	4.40 kg
Coarse aggregate (4.75–12.5 mm)	11.50 kg
Coarse aggregate (12.5–25 mm)	44.50 kg
Normal sand	20.00 kg
Fine sand	20.00 kg
Water	8.00 kg
Retarder 0.5%	51.5 ml
Superplasticizer	51.5 ml
Steel fiber volume ratio and weight	2% ≈ 5.23 kg

terms of compressive strength and ductility (represented by the ultimate compressive strain of concrete). The effect of confinement in concrete is very important to be incorporated (confining parameter Z_m) when analyzing its compressive behavior since it is completely different from that of the unconfined concrete:

$$Z_m = \frac{0.625}{\left[(3 + 0.29 f'_c)/145 \cdot f'_c - 1000\right] + (3/4) \cdot \rho_s \cdot \sqrt{(h''/s_h)} - 0.002K}, \quad (5)$$

$$K = 1.25\left(1 + \frac{\rho_s \cdot f_{yh}}{f'_c}\right), \quad (6)$$

$$\rho_{s1} = 0.12\left(\frac{f'_c}{f_{yh}}\right), \quad (7)$$

$$\rho_{s2} = 0.45\left(\frac{A_g}{A_{ch}} - 1\right)\frac{f'_c}{f_{yh}}, \quad (8)$$

where Z_m is the confining parameter of confined concrete (modified Kent–Park [12]), ρ_s is the volumetric ratio of spiral to the confined concrete core measured outer to outer of spiral, h'' is the width of confined concrete core measured outer to outer of spiral, s_h is the spacing of spiral measured center to center of spiral, K is the multiplying factor, f_{yh} is the yield strength of spiral, A_g is the gross area of concrete section, and A_{ch} is the area of concrete core spirally confined with steel bars [19, 20] measured outer to outer of spiral.

2.3. Specimen Details. The details and cross section of the specimens are illustrated in Figure 2. The specimens listed in Table 2 were designed based on (5)–(8).

3. Test Method

The compressive strength and shortening deformation of concrete cylinders are the main parameters observed in the study. The value of f'_c was obtained from the compressive strength tests of the standard plain concrete cylinders (150 × 300 mm) (without steel fiber) at the age of 28 days after the curing period.

3.1. Test Setup. The test setup to perform the compressive test is shown in Figure 3. The test was carried out until the concrete specimens failed in the compressive crushing mode. The data collected during the tests were the compressive load and shortening until the failure of the specimens. The compressive pressure was generated from the universal testing machine (UTM) with a maximum capacity of 100 tons, and the load was read by the load cell (maximum capacity of 100 tons). For measuring the shortening displacements, a pair of LVDTs was installed at the two opposite sides of the specimen to average the values. All the measurements were transferred to the data logger or universal recorder (UR), and the data were recorded and displayed in the computer.

3.2. Test Procedure. The experimental tests were conducted in the laboratory. First, the course and fine aggregates were evaluated for their compliances with the ASTM standards for normal-strength concrete. The cement used was OPC. Then, the mix design can be calculated and mixed in the laboratory including the curing process until 28 days. The loading type applied to the concrete cylinder specimens was the static monotonic compressive loading. Tensile tests were also carried out for all the steel bars used for spirals as confinement in concrete. Based on the mix design and using the selected materials as mentioned previously, the spirals that have been prepared earlier were cast to produce the concrete cylinders specimen as shown in details in Figure 2. After curing for 28 days, the molds of the specimens were removed and left to dry in the air for a few hours before they were ready for loading tests. The compressive test was conducted until the specimens failed in a crushing manner. From the tests, all the data were collected such as loads and displacements to calculate the compressive stresses and strains of the specimens. The loading was terminated when the spiral has ruptured.

4. Results and Discussion

4.1. Compressive Strength. Tables 3 and 4 show the compressive strength test results of the specimens with and without steel fiber, respectively. Concrete with and without steel fiber confirms that there is an insignificant difference in terms of compressive strength. In fact, all of them tend to similarly approach the target compressive strength of

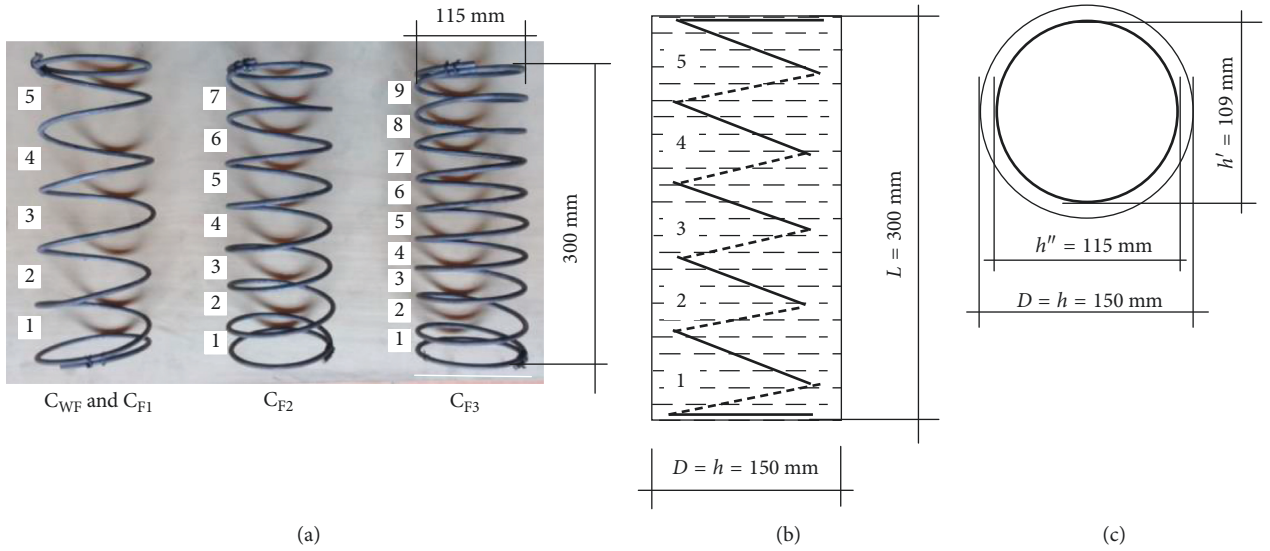

Figure 2: Details of spiral and specimens: (a) details of spiral, (b) dimensions of spirally confined specimens, and (c) cross section of specimens.

Table 2: Details of test specimens.

Specimen ID	D (mm)	L (mm)	Stirrup		V_f	f'_c (MPa)	f_{yh} (MPa)	ρ_{s1}	ρ_{s2}	ρ_s used	Z_m
			ϕ (mm)	s_h (mm)							
C_{WF}	150	300	6	52	0	22.5	457	0.0059	0.0155	0.0189	28.625
C_{F1}	150	300	6	52	2%	22.5	457	0.0059	0.0155	0.0189	28.625
C_{F2}	150	300	6	36	2%	22.5	457	0.0059	0.0155	0.0273	16.926
C_{F3}	150	300	6	27	2%	22.5	457	0.0059	0.0155	0.0364	11.118

Note. C_{WF} is the spirally confined concrete cylinder without steel fiber, C_{Fn} is the spirally confined concrete cylinder with steel fiber, D is the cylinder diameter, and L is the cylinder height.

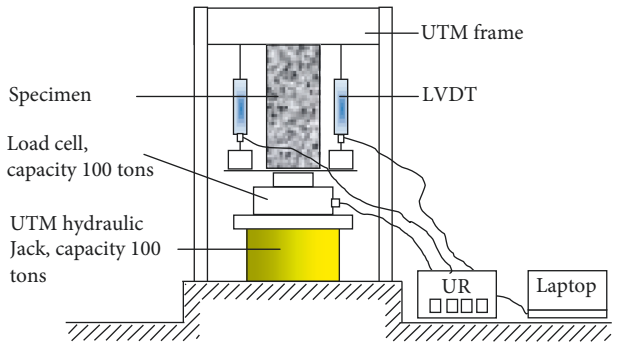

Figure 3: Schematic of test setup. UR = universal recorder; LVDT = linear variable displacement transducer.

Table 3: Unconfined concrete specimens without steel fiber.

Specimen ID	ε_c	f'_c (MPa)
C_1	0.00246	23.0892
C_2	0.00239	23.1069
Average	0.00243	23.0981

Table 4: Unconfined concrete specimens with steel fiber.

Specimen ID	ε_c	f'_c (MPa)
C_3	0.00391	23.1016
C_4	0.00207	23.4253
Average	0.00299	23.2634

concrete (f'_c) of 22.5 MPa. Thus, it can be concluded that the addition of steel fiber did not affect the compressive strength of concrete significantly [15]. The test results can be seen in Tables 3 and 4.

4.2. Maximum Compressive Stress. The maximum compressive stresses of each concrete specimen from the experimental results can be obtained from their corresponding stress-strain curves. It can be seen that the maximum compressive strengths of all specimens vary with the variation of volumetric ratio of spiral and steel fiber. Based on the calculated volumetric ratios of the spiral as confinement, the values of Z_m can also be obtained, namely, $Z_{m1} = 28.625$, $Z_{m2} = 16.926$, and $Z_{m3} = 11.118$ for specimens C_{F1}, C_{F2}, and C_{F3}, respectively. The compressive strengths of spirally confined concretes without steel fiber can reach up to $f_{C_{WF}} = 24.0269$ MPa, while for those with steel fiber can reach up to $f_{C_{F1}} = 26.0262$ MPa, $f_{C_{F2}} = 29.2993$ MPa, and $f_{C_{F3}} = 33.4394$ MPa (Figure 4).

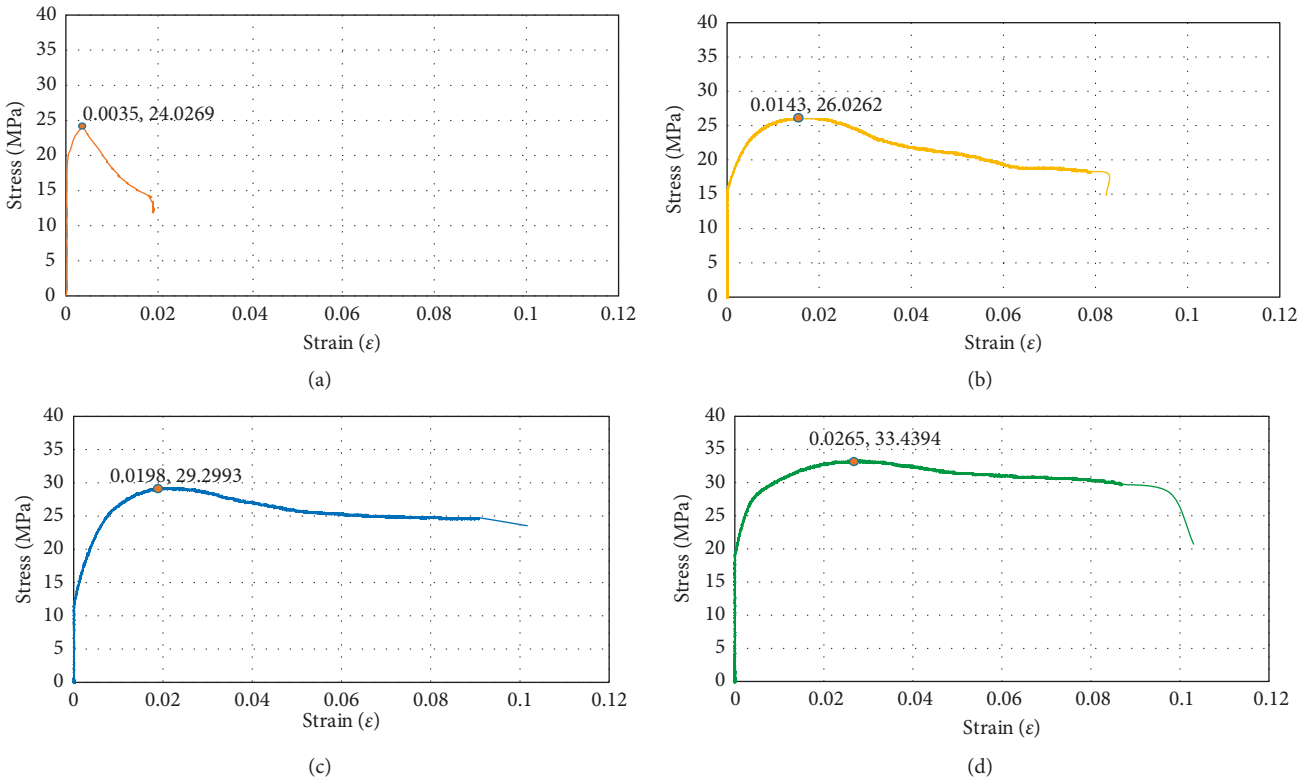

FIGURE 4: Experimental stress-strain curves of test specimens: (a) specimen C_{WF} ($Z_{mWF} = 28.625$), (b) specimen C_{F1} ($Z_{m1} = 28.625$), (c) specimen C_{F2} ($Z_{m2} = 16.926$), and (d) specimen C_{F3} ($Z_{m3} = 11.118$).

4.3. Failure Modes. The failure modes indicated the combined effect of steel fiber and spiral as confinement. All the test specimens failed in their midheights as shown in Figure 5. The plain concrete cylinder specimen performed a brittle sudden failure. For spirally confined specimens, it indicated better performance (more ductile) as the failures of the specimens can be delayed slowly in the postpeak responses. The failures of the specimens were obtained when the steel spirals were ruptured. The specimens with steel fiber failed at the compressive strains in the range of $0.0823 < \varepsilon_c < 0.1031$, whereas the compressive stresses were in the range of $14.826 < f_c < 23.549$ MPa. When compared to the unconfined concrete without steel fiber (plain concrete), its failure occurred when the strain and stress were $\varepsilon_c = 0.018$ and $f_c = 11.818$ MPa, respectively.

4.4. Ductility. From the experimental results, it can be seen that the spirally confined specimens with steel fiber indicated very ductile failure manners. At the loading of a half of P_{max}, they showed low degradation of stiffness. In the postpeak responses, they performed better strain ductility compared to that without steel fiber. The increase in strain ductility is due to the combined effect of spiral and steel fiber [12]. However, from the experimental results, it indicates that the steel fiber contributes significantly to the tensile strength of concrete, and consequently, the strain ductility of the concrete also increases considerably. The comparison of the experimental stress-strain curves of the specimens with various confinement ratios is shown in Figure 6.

4.5. Effect of Confining Parameter Z_m. The confining parameter Z_m [12] was adopted to consider the effect of confinement of the specimens. The value of Z_m is very crucial in the determination of confinement of the specimens. If the value of Z_m is known, then the value of s_h (spiral's pitch) can be found, or vice versa; if the spiral's pitch is known, then the value of Z_m can be obtained. Better concrete confinement can be achieved by lowering the value of Z_m. To reduce the value of Z_m, ρ_s can be increased. The greater the value of ρ_s, the better confining effect to the concrete core such that the value of Z_m is lower. Thus, the lower the value of Z_m, the better the ductility of the concrete (longer ultimate compressive strain). The study confirmed the phenomenon. With the lowest value of Z_m equal to 11.118, the concrete specimen is capable of attaining an ultimate compressive strain of 0.1031 with a slightly descending slope.

4.6. Proposed Model. Assuming that the compressive strength of concrete without steel fiber equals to that of concrete with steel fiber, Equations (9)–(11) were proposed in the study. The comparison of the peak stresses and the corresponding strains at peak stresses between the proposed

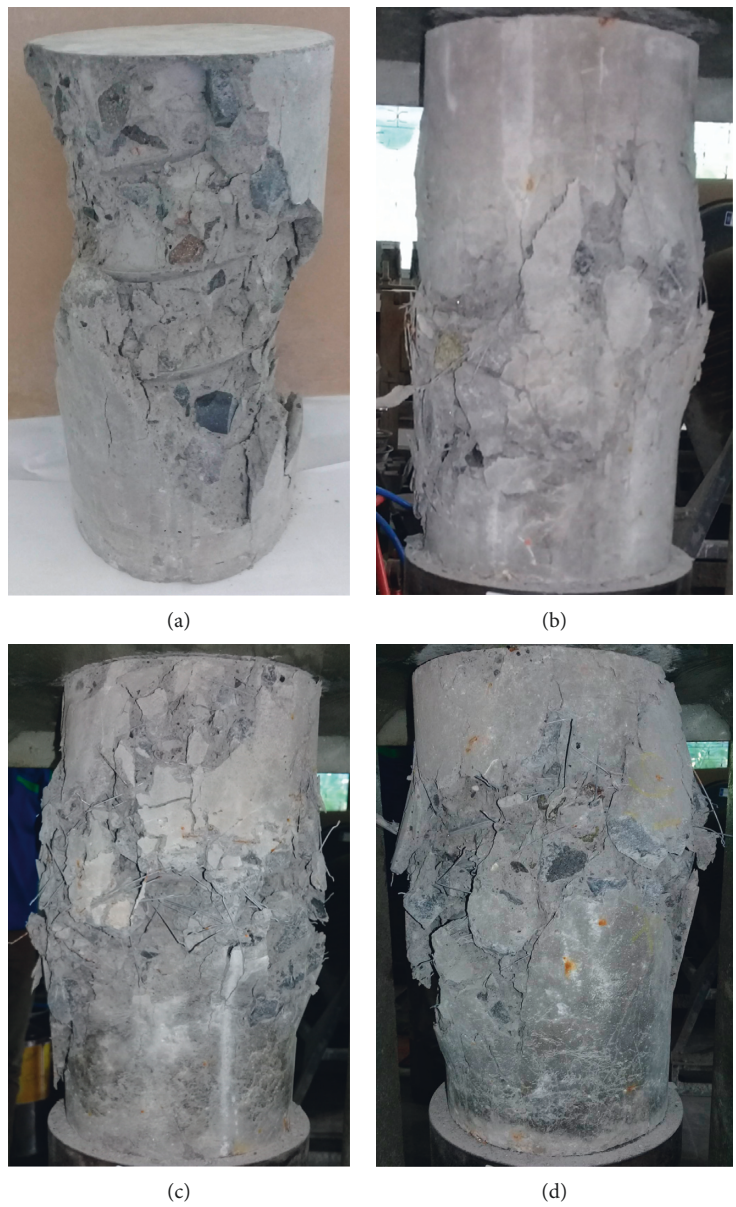

Figure 5: Failure modes of all specimens after completion of the tests: (a) specimen C_{WF}, (b) specimen C_{F1}, (c) specimen C_{F2}, and (d) specimen C_{F3}.

equations and the experimental results is given in Figure 7 and Tables 5 and 6. The comparison of the strains at failures between the proposed equations and the experimental results is given in Table 7. The increases of stresses and strains are also listed in Tables 8 and 9.

The proposed equations developed based on the data obtained from the experimental tests in the study are given as follows:

$$f'_{cfc} = f'_{cc} + \frac{57I_f}{Z_m}, \tag{9}$$

$$\varepsilon_{pfc} = \varepsilon_{cc} + \frac{0.1747I_f}{Z_m}, \tag{10}$$

$$\varepsilon_{ffc} = \varepsilon_{pfc} + \frac{0.95I_f}{Z_m}, \tag{11}$$

where f'_{cfc} is the compressive strength of spirally confined SFRC, f'_{cc} is the compressive strength of spirally confined non-SFRC, ε_{pfc} is the strain corresponding to the peak stress of spirally confined SFRC, ε_{cc} is the strain corresponding to the peak stress of spirally confined non-SFRC = 0.0035, ε_{ffc} is the strain at failure of spirally confined SFRC, and ε_{pfc} is the strain corresponding to the peak stress of spirally confined SFRC. The proposed equations (9)–(11) can be used for predicting the compressive behavior of SFRC (2 percent) spirally confined with various volumetric ratio of steel bars.

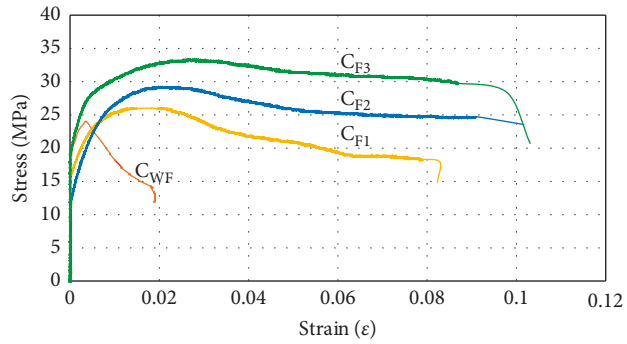

Figure 6: Comparison of experimental stress-strain curves of the specimen with various confinement ratios.

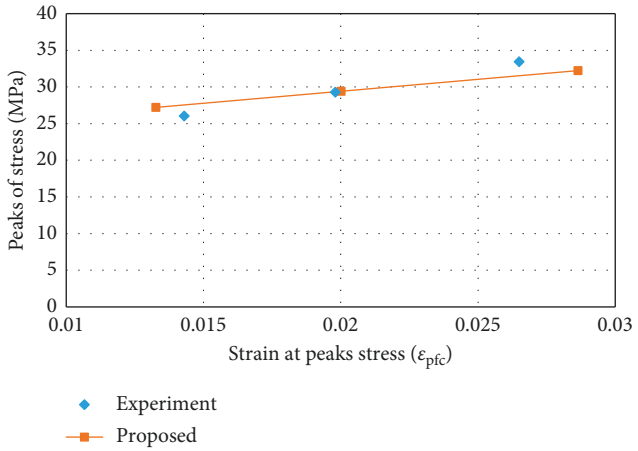

Figure 7: Comparison of peak stress versus strain at peak stress between the proposed and experimental results.

Table 5: Comparison of peak stresses between the proposed and experimental results.

Specimen ID	Experiment f'_{cfc} (MPa)	Proposed (9) f'_{cfc} (MPa)	Δ_f (MPa)
C_{F1}	26.0262	27.2129	1.1867
C_{F2}	29.2993	29.4151	0.1158
C_{F3}	33.4394	32.2298	−1.2096

Table 6: Comparison of strains at peak stresses between the proposed and experimental results.

Specimen ID	Experiment ε_{pfc}	Proposed (10) ε_{pfc}	Δ_ε
C_{F1}	0.0143	0.0133	−0.0010
C_{F2}	0.0198	0.0200	0.0002
C_{F3}	0.0265	0.0286	0.0021

5. Conclusions

Based on the discussion above, it can be concluded that due to the use of combination of steel fiber and spiral as confinement in concrete, both the stress and the strain of concrete increases, and thus, it becomes more ductile. The peak stress of the concrete can increase up to 39.17 percent, while the strain value can increase up to 657.14 percent (when it is compared to the ultimate strain of plain or unconfined concrete which is considered about 0.0035). The unconfined concrete behavior performed significantly different behavior with the confined concrete where the confined concrete indicated much more ductile behavior than the unconfined concrete. In the study, the peak stress and the corresponding strain at peak stress can be well predicted with the proposed equations particularly for the spirally confined concrete with steel fiber. The proposed equations include parameter Z_m to consider the combined effect of spiral and steel fiber.

Table 7: Comparison of strains at failures between the proposed and experimental results.

Specimen ID	Experiment ε_{ffc}	Proposed (11) ε_{ffc}	Δ_ε
C_{F1}	0.0823	0.0566	−0.0257
C_{F2}	0.1016	0.0933	−0.0083
C_{F3}	0.1031	0.1402	0.0372

Table 8: Increase of peak stresses.

Specimen ID	f'_{cc} (MPa)	f'_{cfc} (MPa)	Increase from f'_{cc}
C_{WF}	24.0269	—	—
C_{F1}	—	26.0262	8.32%
C_{F2}	—	29.2993	21.94%
C_{F3}	—	33.4394	39.17%

Table 9: Increase of strains at peak stresses.

Specimen ID	ε_{cc}	ε_{pfc}	Increase from ε_{cc}
C_{WF}	0.0035	—	—
C_{F1}	—	0.0143	307.58%
C_{F2}	—	0.0198	465.71%
C_{F3}	—	0.0265	657.14%

Conflicts of Interest

The authors declare that there are no conflicts of interest regarding the publication of this paper.

References

[1] T. Tavio, B. Kusuma, and P. Suprobo, "Experimental behavior of concrete columns confined by welded wire fabric as transverse reinforcement under axial compression," *ACI Structural Journal*, vol. 109, no. 3, pp. 339–348, 2012.

[2] B. Kusuma, T. Tavio, and P. Suprobo, "Statistical analysis of confined columns with varying reinforcement configuration and ratios," in *Proceedings of the International Conference on Environmentally Friendly Civil Engineering Construction and Materials (EFCECM-2014): Creating and Adapting Sustainable Technologies*, pp. 141–154, Manado, Indonesia, November 2014.

[3] T. Tavio, P. Suprobo, and B. Kusuma, "Strength and ductility enhancement of reinforced HSC columns confined with high-strength transverse steel," in *Proceedings of the Eleventh East Asia-Pacific Conference on Structural*

Engineering and Construction (EASEC-11), pp. 350-351, Taipei, Taiwan, November 2008.

[4] B. Kusuma and T. Tavio, "Unified stress-strain model for confined columns of any concrete and steel strengths," in *Proceedings of the International Conference on Earthquake Engineering and Disaster Mitigation (ICEEDM-I)*, pp. 502–509, Jakarta, Indonesia, April 2008.

[5] P. Pudjisuryadi, T. Tavio, and P. Suprobo, "Axial compressive behavior of square concrete columns externally collared by light structural steel angle sections," *International Journal of Applied Engineering Research*, vol. 11, no. 7, pp. 4655–4666, 2016.

[6] P. Pudjisuryadi, T. Tavio, and P. Suprobo, "Performance of square reinforced concrete columns externally confined by steel angle collars under combined axial and lateral load," *Procedia Engineering*, vol. 125, pp. 1043–1049, 2015.

[7] T. Tavio, P. Suprobo, and B. Kusuma, "Ductility of confined reinforced concrete columns with welded reinforcement grids," *Excellence in Concrete Construction through Innovation–Proceedings of the International Conference on Concrete Construction*, pp. 339–344, CRC Press, Taylor and Francis Group, London, UK, 2009.

[8] B. Kusuma, T. Tavio, and P. Suprobo, "Axial load behavior of concrete columns with welded wire fabric as transverse reinforcement," *Procedia Engineering*, vol. 14, pp. 2039–2047, 2011.

[9] T. Tavio, B. Kusuma, and P. Suprobo, "Investigation of stress-strain models for confinement of concrete by welded wire fabric," *Procedia Engineering*,vol. 14, pp. 2031–2038, 2011.

[10] T. Tavio and B. Kusuma, "Stress-strain model for high-strength concrete confined by welded wire fabric," *Journal of Materials in Civil Engineering*, vol. 21, no. 1, pp. 40–45, 2009.

[11] A. S. Ezeldin and P. N. Balaguru, "Normal and high-strength fiber reinforced concrete under compression," *Journal of Materials in Civil Engineering*, vol. 4, no. 4, pp. 415–429, 1992.

[12] B. D. Scott, R. Park, and M. J. N. Priestley, "Stress-strain behavior of concrete confined by overlapping hoops at low and high strain rates," *ACI Journal*, vol. 79, no. 1, pp. 13–27, 1982.

[13] M. C. Nataraja, N. Dhang, and A. P. Gupta, "Stress strain curve for steel-fiber reinforced concrete under compression," *Cement and Concrete Composites*, vol. 21, no. 5-6, pp. 383–390, 1999.

[14] R. P. Dhakal, C. Wang, and J. B. Mander, *Behavior of Steel Fibre Reinforced Concrete in Compression*, UC Research Repository, University Library, University of Canterbury, Christchurch, New Zealand, 2017, http://hdl.handle.net/10092/4408.

[15] L. A. D. Oliveira Júnior, V. E. dos Santos Borges, A. R. Danin et al., "Stress-strain curves for steel fiber-reinforced concrete in compression," *Matéria (Rio de Janeiro)*, vol. 15, no. 2, pp. 260–266, 2010.

[16] P. Soroushian and C. D. Lee, "Constitutive modeling of steel fiber reinforced concrete under direct tension and compression," in *Fibre Reinforced Cements and Concretes, Recent Developments*, R. N. Swamy and B. Barr, Eds., pp. 363–375, CRC Press, Boca Raton, FL, USA, 1989.

[17] Y. C. Ou, M. S. Tsai, K. Y. Liu, and K. C. Chang, "Compressive behavior of steel-fiber-reinforced concrete with a high reinforcing index," *Journal of Materials in Civil Engineering*, vol. 24, no. 2, pp. 207–215, 2012.

[18] C. Liu, *Seismic Behaviour of Beam-Column Joint Subassemblies Reinforced with Steel Fibers*, M.S. thesis, Department of Civil Engineering, University of Canterbury, Christchurch, New Zealand, 2006.

[19] T. Tavio, R. Anggraini, I. G. P. Raka, and A. Agustiar, "Tensile strength/yield strength (TS/YS) ratios of high-strength steel (HSS) reinforcing bars," *AIP Conference Proceedings*, vol. 1964, no. 1, pp. 020036-1–020036-8, 2018.

[20] R. Anggraini, T. Tavio, I. G. P. Raka, and A. Agustiar, "Stress-strain relationship of high-strength steel (HSS) reinforcing bars," *AIP Conference Proceedings*, vol. 1964, no. 1, pp. 020025-1–020025-8, 2018.